

PREPARATION AND OPERATIONS OF THE MISSION PERFORMANCE  
CENTRE (MPC) FOR THE COPERNICUS SENTINEL-3 MISSION

**S3-A SLSTR Cyclic Performance Report**

**Cycle No. 023**

**Start date: 30/09/2017**

**End date: 27/10/2017**



*Mission  
Performance  
Centre*



**Ref.:** S3MPC.RAL.PR.02-023  
**Issue:** 1.0  
**Date:** 06/11/2017  
**Contract:** 400011836/14/I-LG

<b>Customer:</b> ESA	<b>Document Ref.:</b> S3MPC.RAL.PR.02-023
<b>Contract No.:</b> 4000111836/14/I-LG	<b>Date:</b> 06/11/2017
	<b>Issue:</b> 1.0

<b>Project:</b>	PREPARATION AND OPERATIONS OF THE MISSION PERFORMANCE CENTRE (MPC) FOR THE COPERNICUS SENTINEL-3 MISSION		
<b>Title:</b>	S3-A SLSTR Cyclic Performance Report		
<b>Author(s):</b>	SLSTR ESLs		
<b>Approved by:</b>	D. Smith, SLSTR ESL Coordinator	<b>Authorized by</b>	Frédéric Rouffi, OPT Technical Performance Manager
<b>Distribution:</b>	ESA, EUMETSAT, S3MPC consortium		
<b>Accepted by ESA</b>	S. Dransfeld, MPC Deputy TO for OPT  P. Féménias, MPC TO		
<b>Filename</b>	S3MPC.RAL.PR.02-023 - i1r0 - SLSTR Cyclic Report 023.docx		

#### Disclaimer

The work performed in the frame of this contract is carried out with funding by the European Union. The views expressed herein can in no way be taken to reflect the official opinion of either the European Union or the European Space Agency.







## Table of content

<b>1</b>	<b>INSTRUMENT MONITORING .....</b>	<b>1</b>
1.1	INSTRUMENT TEMPERATURES.....	1
1.2	SCANNER PERFORMANCE .....	5
1.3	DETECTOR NOISE LEVELS .....	7
1.3.1	<i>VIS and SWIR channel signal-to-noise</i> .....	7
1.3.2	<i>TIR channel NEDT</i> .....	9
1.4	CALIBRATION FACTORS .....	11
1.4.1	<i>VIS and SWIR VISCAL signal response</i> .....	11
<b>2</b>	<b>LEVEL 2 SST VALIDATION .....</b>	<b>13</b>
2.1	DEPENDENCE ON LATITUDE, TCWV, SATELLITE ZA AND DATE .....	13
2.2	SPATIAL DISTRIBUTION OF MATCH-UPS.....	14
2.3	MATCH-UPS STATISTICS .....	15
<b>3</b>	<b>LEVEL 2 LST VALIDATION .....</b>	<b>16</b>
3.1	CATEGORY-A VALIDATION .....	16
3.2	CATEGORY-C VALIDATION .....	18
<b>4</b>	<b>EVENTS .....</b>	<b>19</b>
<b>5</b>	<b>APPENDIX A .....</b>	<b>20</b>

## List of Figures

Figure 1: Detector temperatures for each channel from 1st March 2016. Discontinuities occur for the infrared channels where the FPA was heated for decontamination or following an anomaly. The vertical dashed lines indicate the start and end of each cycle. ----- 1

Figure 2: Blackbody temperature and baseplate gradient trends. The vertical dashed lines indicate the start and end of each cycle. ----- 2

Figure 3: Baffle temperature trends. The vertical dashed lines indicate the start and end of each cycle. - 3

Figure 4: Opto-Mechanical Enclosure (OME) temperature trends showing the paraboloid stops and flip baffle (top two plots) and optical bench and scanner and flip assembly (lower two plots). The top two plots only show data starting from 30th July 2016. The vertical dashed lines indicate the start and end of each cycle. ----- 4

Figure 5: Scanner and flip jitter, showing mean, stddev and max/min position compared to the expected one for the nadir view. The vertical dashed lines indicate the start and end of each cycle. ----- 5

Figure 6: Scanner and flip jitter, showing mean, stddev and max/min position compared to the expected one for the oblique view. The vertical dashed lines indicate the start and end of each cycle. ----- 6

Figure 7: VIS and SWIR channel signal-to-noise of the measured VISCAL signal in each orbit. Different colours indicate different detectors. ----- 8

Figure 8: NEDT trend for the thermal channels. Blue points were calculated from the cold blackbody signal and red points from the hot blackbody. Horizontal lines indicate the requirement (dashed) and goal (dotted) as well as the measured values on ground (red and blue dashed). ----- 9

Figure 9: VISCAL signal trend for VIS channels (nadir view). -----11

Figure 10: VISCAL signal trend for SWIR channels (nadir view).-----12

Figure 11: Dependence of median and robust standard deviation of match-ups between SLSTR SST<sub>skin</sub> and drifting buoy SST<sub>depth</sub> for Cycle 23 as a function of latitude, total column water vapour (TCWV), satellite zenith angle and date. The data gap towards the end of the cycle is due to a delay in match-up production. -----13

Figure 12: Spatial distribution of match-ups between SLSTR SST<sub>skin</sub> and drifting buoy SST<sub>depth</sub> for Cycle 23.14

Figure 13: Validation of the SL\_2\_LST product over the mid-July to mid-November reprocessed period at three Gold Standard in situ stations managed by the Karlsruhe Institute of Technology: Evora, Portugal (left); Gobabeb, Namibia (centre); Kalahari-Heimat, Namibia (right). [Results courtesy of Maria Martin through the GlobTemperature Project]-----16

Figure 14: Validation of the SL\_2\_LST product over the mid-July to mid-November reprocessed period at the seven Gold Standard in situ stations of the SURFRAD network plus a Gold Standard station from the ARM network: Bondville, Illinois top-(left); Desert Rock, Nevada (top-centre); Fort Peck, Montana (top-right); Goodwin Creek, Mississippi (middle-left); Penn State University, Pennsylvania (middle-centre); Sioux Fall, South Dakota (middle-right); Table Mountain, Colorado (bottom-left); and Southern Great Plains, Oklahoma (bottom-centre). -----17

	<p><b>Sentinel-3 MPC</b></p> <p><b>S3-A SLSTR Cyclic Performance Report</b></p> <p><b>Cycle No. 023</b></p>	<p>Ref.: S3MPC.RAL.PR.02-023</p> <p>Issue: 1.0</p> <p>Date: 06/11/2017</p> <p>Page: vi</p>
--	---	--

Figure 15: Level-1 image for visible channels (left) with S1 blue, S2 green and S3 red, and for S8 (right) on 25<sup>th</sup> October 2017 for the granule starting at 10:30. The affected area starts at 10:31 in the visible channels and at 10:33 in the infrared channels. -----19

**List of Tables**

Table 1: Average reflectance factor, and signal-to-noise ratio of the measured VISCAL signal for cycles 012-023, averaged over all detectors for the nadir view. ----- 7

Table 2: Average reflectance factor, and signal-to-noise ratio of the measured VISCAL signal for cycles 012-023, averaged over all detectors for the oblique view. ----- 7

Table 3: NEDT for cycles 012-023 averaged over all detectors for both Earth views towards the +YBB (hot). -----10

Table 4: NEDT for cycles 012-023 averaged over all detectors for both Earth views towards the -YBB (cold). -----10

Table 5: SLSTR drifter match-up statistics for Cycle 23. -----15



# 1 Instrument monitoring

## 1.1 Instrument temperatures

- ❖ Instrument temperatures were stable and consistent with expected values following the decontamination phase which was performed towards the end of Cycle 20.
- ❖ In Cycle 23, blackbody, baffle and OME temperatures were at their expected values, beginning to rise as the Earth approaches perihelion. Gradients across the blackbody baseplate are stable and within their expected range.

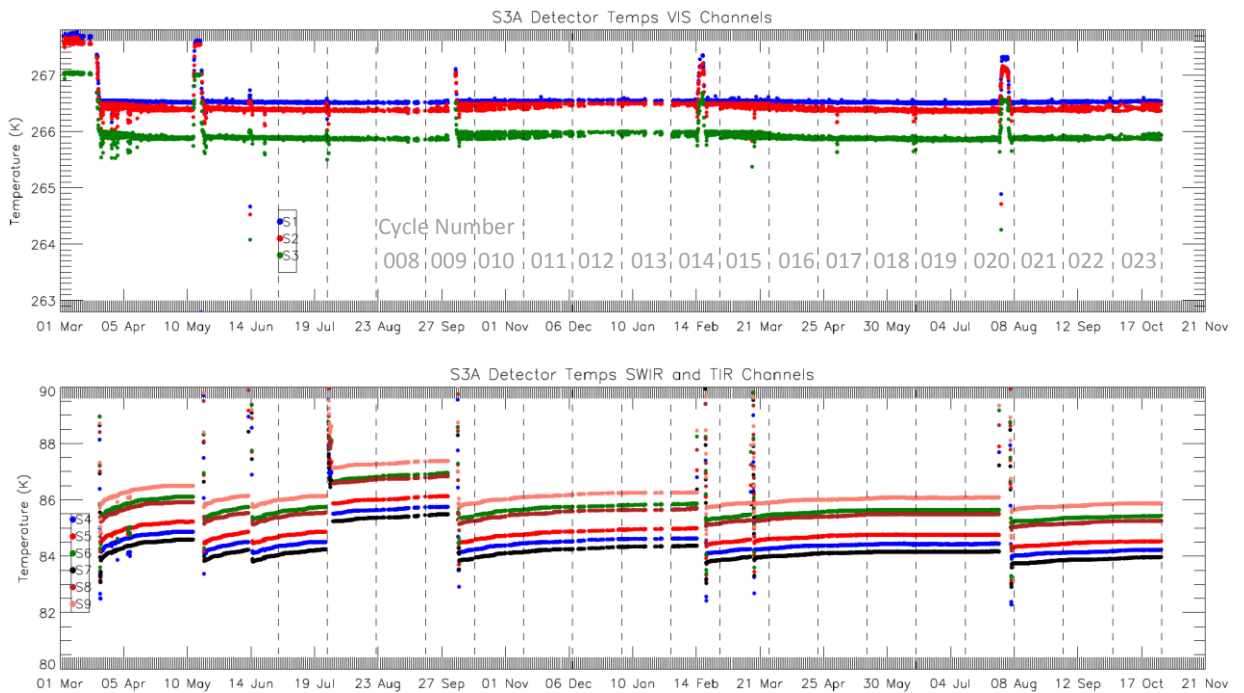


**Figure 1: Detector temperatures for each channel from 1st March 2016. Discontinuities occur for the infrared channels where the FPA was heated for decontamination or following an anomaly. The vertical dashed lines indicate the start and end of each cycle.**



Sentinel-3 MPC  
S3-A SLSTR Cyclic Performance Report  
Cycle No. 023

Ref.: S3MPC.RAL.PR.02-023  
Issue: 1.0  
Date: 06/11/2017  
Page: 2

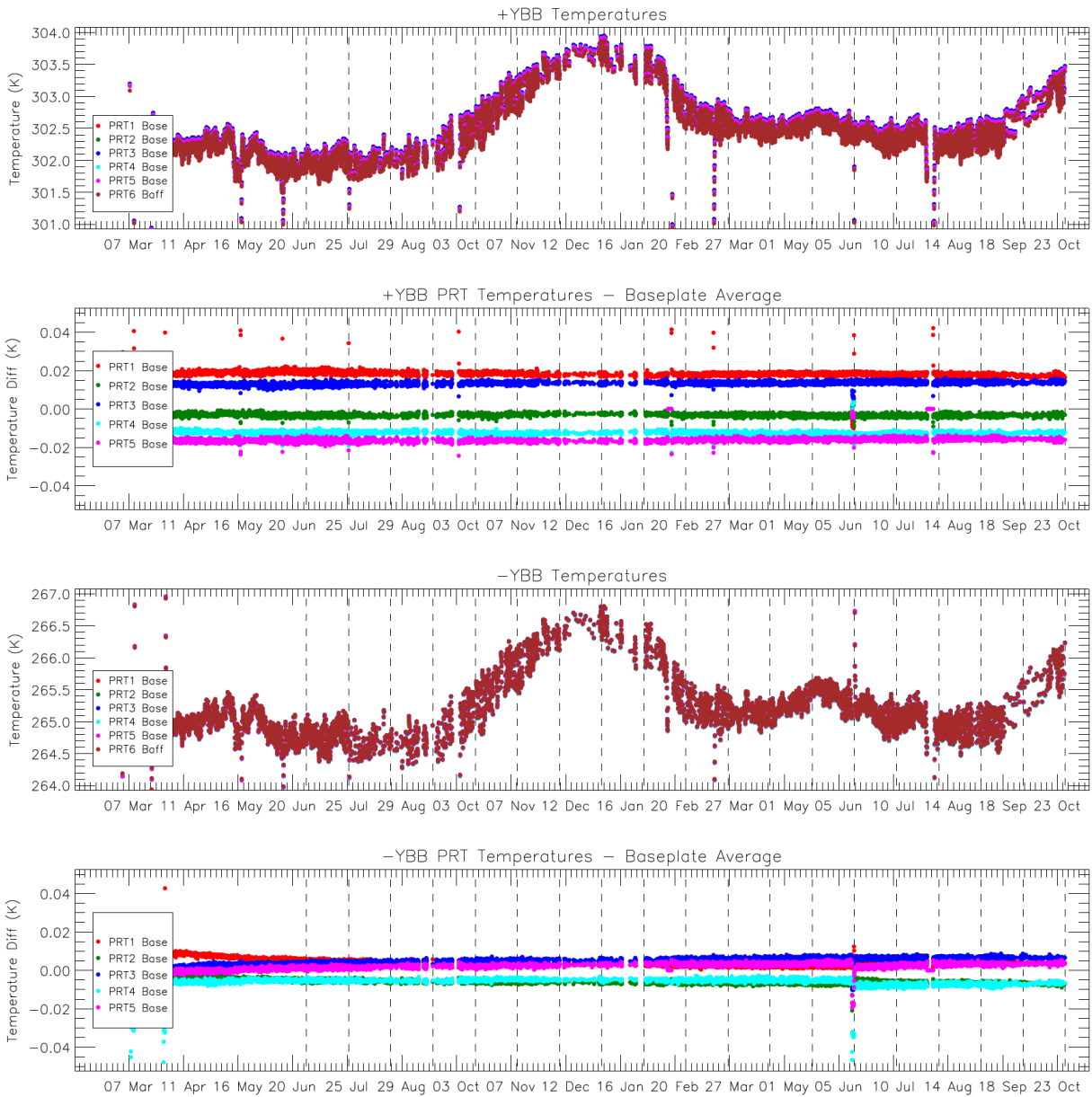


**Figure 2: Blackbody temperature and baseplate gradient trends. The vertical dashed lines indicate the start and end of each cycle.**





Sentinel-3 MPC  
S3-A SLSTR Cyclic Performance Report  
Cycle No. 023

Ref.: S3MPC.RAL.PR.02-023  
Issue: 1.0  
Date: 06/11/2017  
Page: 3

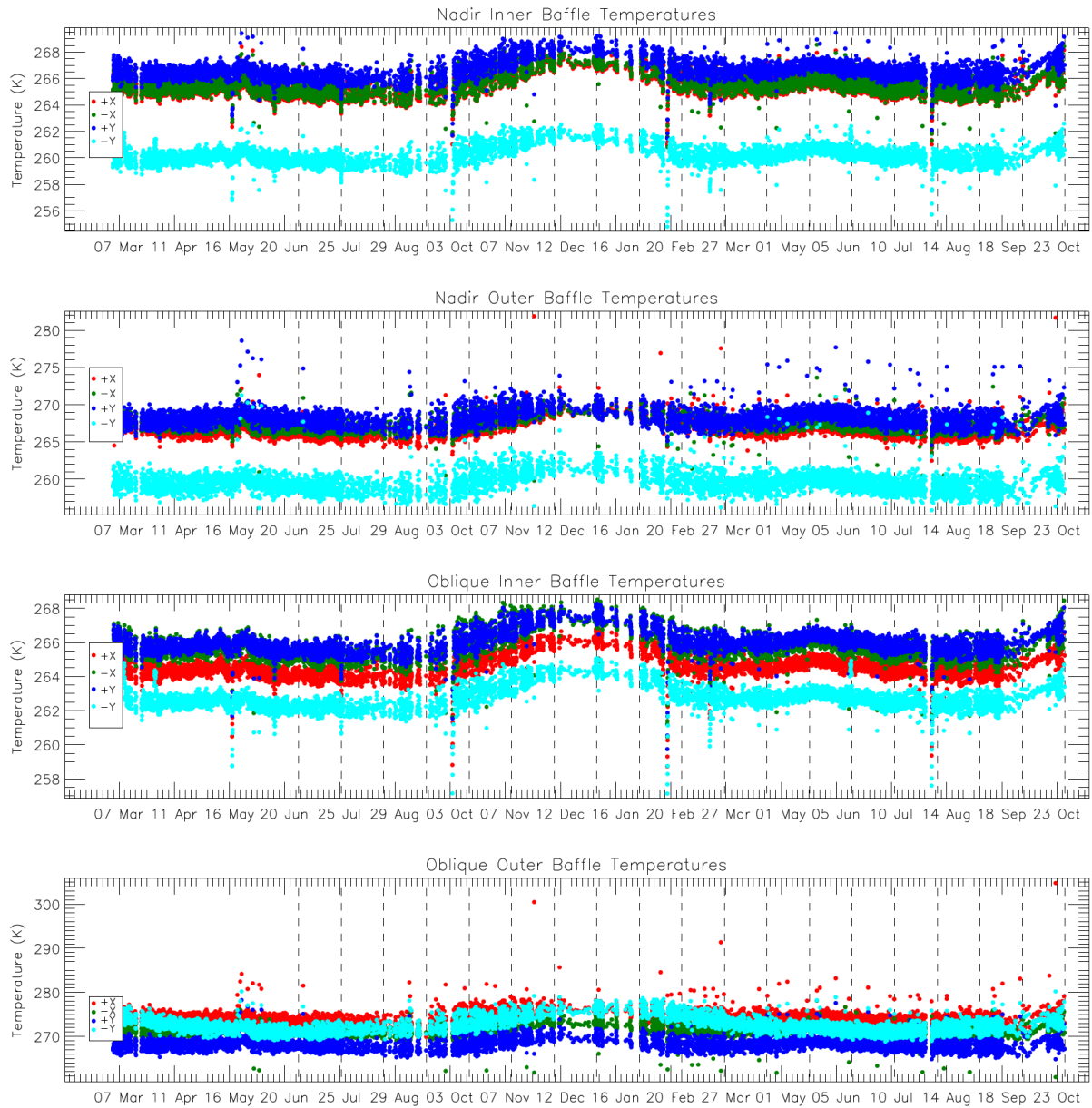
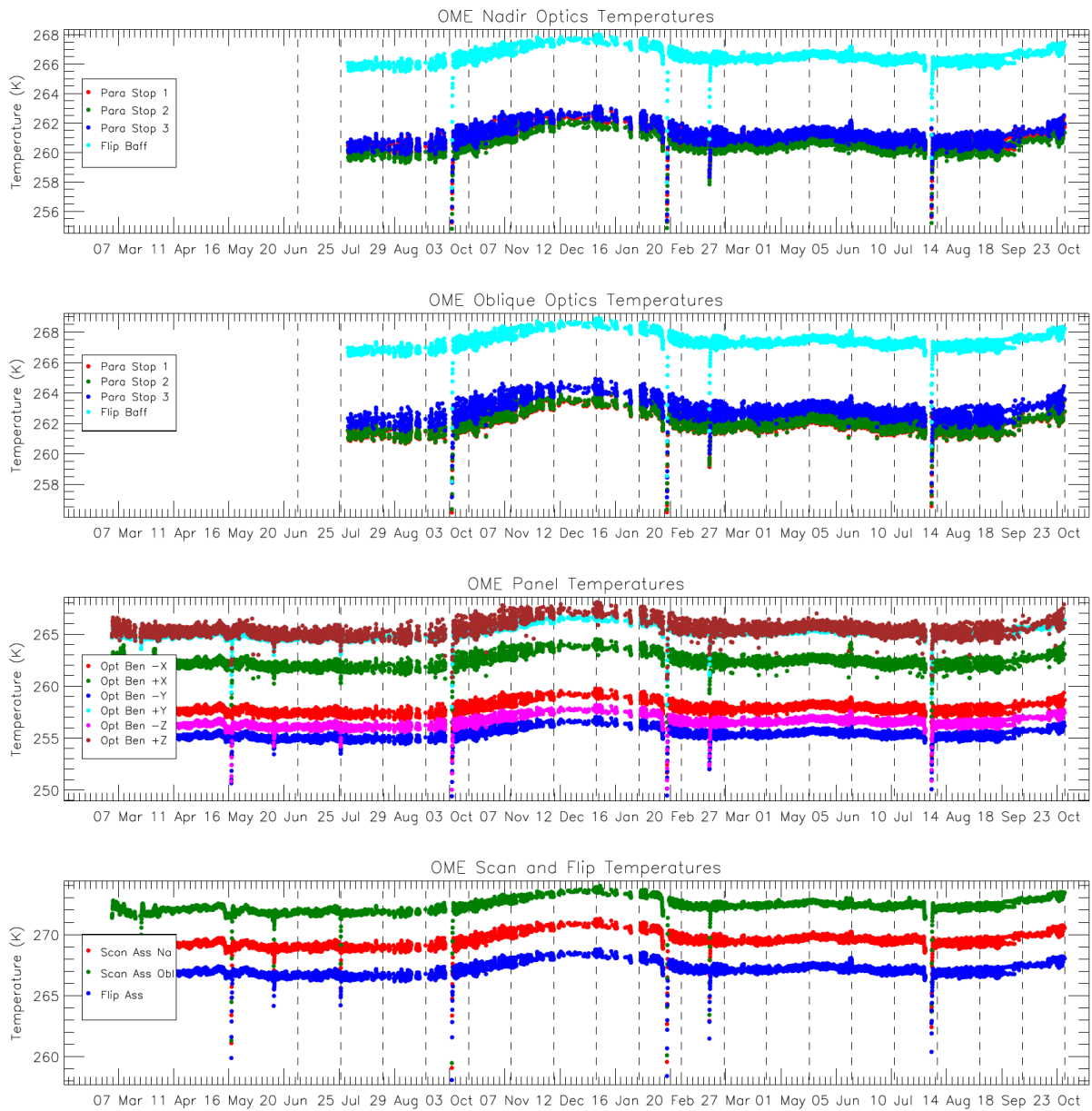


Figure 3: Baffle temperature trends. The vertical dashed lines indicate the start and end of each cycle.



**Figure 4: Opto-Mechanical Enclosure (OME) temperature trends showing the paraboloid stops and flip baffle (top two plots) and optical bench and scanner and flip assembly (lower two plots). The top two plots only show data starting from 30th July 2016. The vertical dashed lines indicate the start and end of each cycle.**



## 1.2 Scanner performance

Scanner performance has been consistent with previous operations and within required limits.

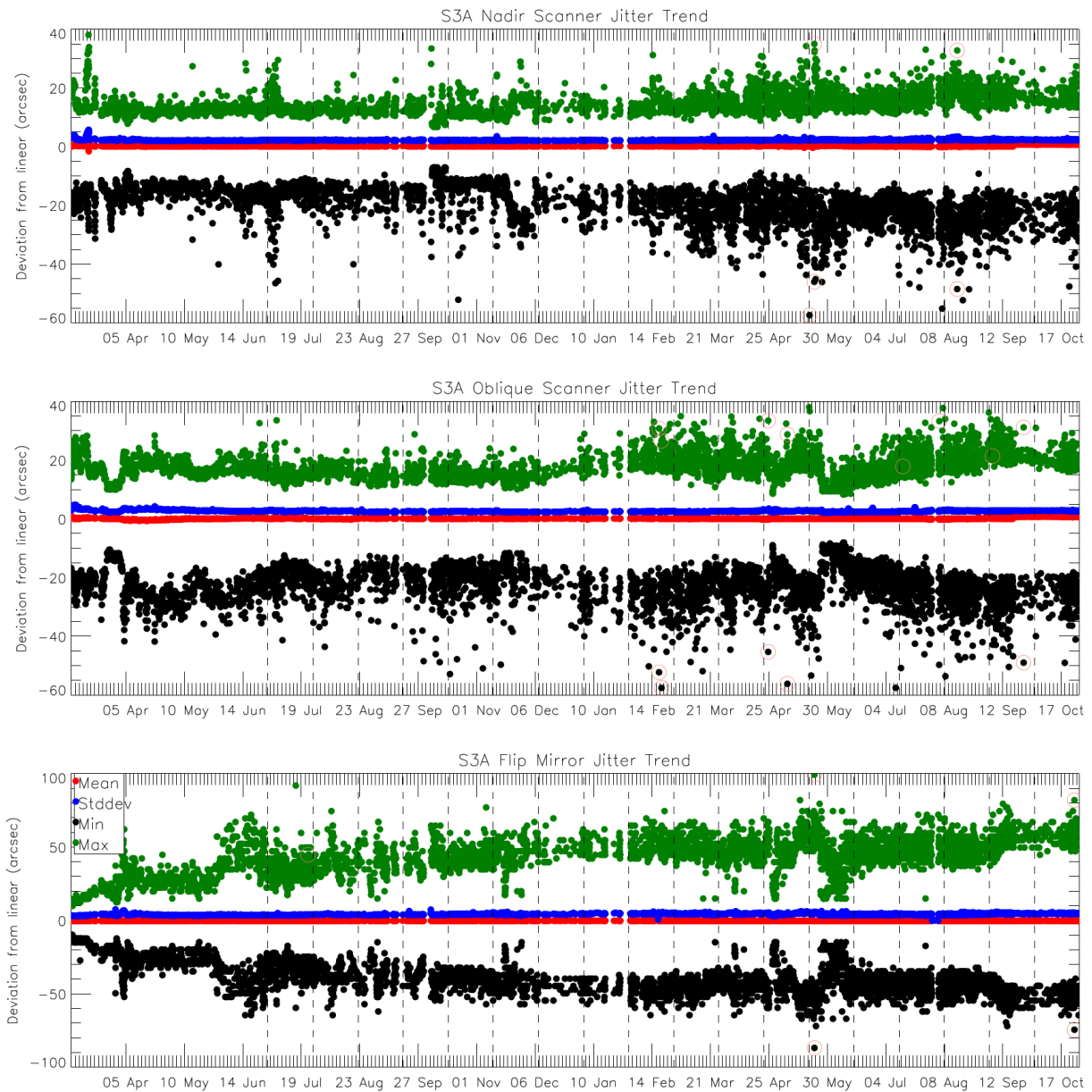


**Figure 5: Scanner and flip jitter, showing mean, stddev and max/min position compared to the expected one for the nadir view. The vertical dashed lines indicate the start and end of each cycle.**

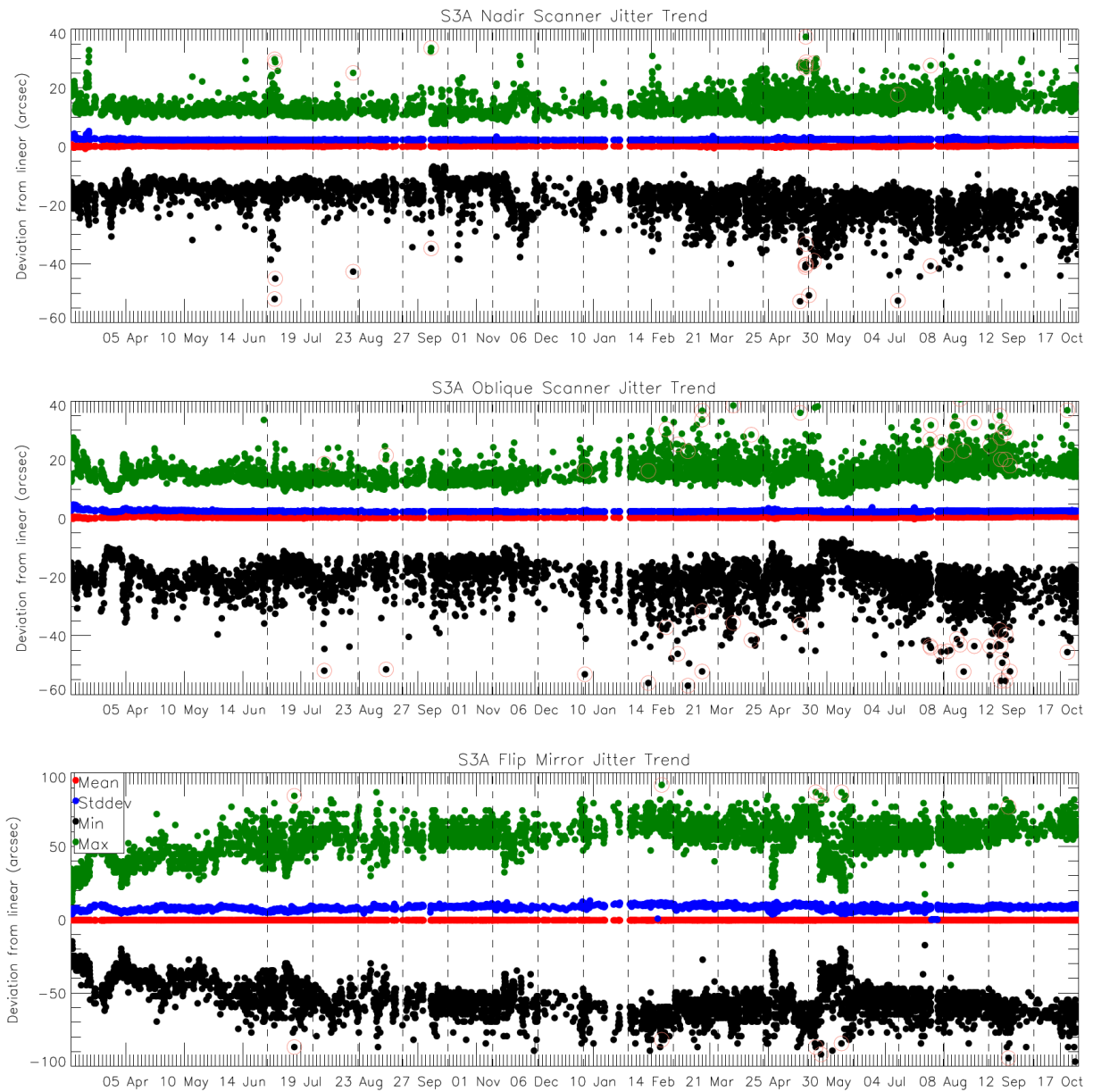


Figure 6: Scanner and flip jitter, showing mean, stddev and max/min position compared to the expected one for the oblique view. The vertical dashed lines indicate the start and end of each cycle.



### 1.3 Detector noise levels

#### 1.3.1 VIS and SWIR channel signal-to-noise

The VIS and SWIR channel noise was stable and consistent with previous operations - the signal-to-noise ratio of the measured VISCAL signal is plotted in Figure 7. Table 1 and Table 2 give the average signal-to-noise in each cycle (excluding the anomaly/decontamination period in Cycle 20). Note that this averages over the significant detector-detector dispersion for the SWIR channels that is shown in Figure 7.

**Table 1: Average reflectance factor, and signal-to-noise ratio of the measured VISCAL signal for cycles 012-023, averaged over all detectors for the nadir view.**

	Average Reflectance Factor	Nadir Signal-to-noise ratio											
		Cycle 012	Cycle 013	Cycle 014	Cycle 015	Cycle 016	Cycle 017	Cycle 018	Cycle 019	Cycle 020	Cycle 021	Cycle 022	Cycle 023
S1	0.187	233	226	217	224	233	234	231	229	233	231	231	234
S2	0.194	236	234	227	230	236	236	232	231	235	235	234	239
S3	0.190	235	230	221	230	236	238	228	231	230	229	228	234
S4	0.191	141	139	137	139	142	140	140	139	137	135	135	138
S5	0.193	238	234	234	233	233	235	236	233	232	232	230	235
S6	0.175	145	143	141	144	142	143	143	142	140	136	139	142

**Table 2: Average reflectance factor, and signal-to-noise ratio of the measured VISCAL signal for cycles 012-023, averaged over all detectors for the oblique view.**

	Average Reflectance Factor	Oblique Signal-to-noise ratio											
		Cycle 012	Cycle 013	Cycle 014	Cycle 015	Cycle 016	Cycle 017	Cycle 018	Cycle 019	Cycle 020	Cycle 021	Cycle 022	Cycle 023
S1	0.166	247	238	229	236	243	247	246	242	241	241	243	243
S2	0.170	250	241	232	241	248	251	249	247	247	244	244	253
S3	0.168	244	237	227	236	245	249	244	242	239	234	240	247
S4	0.166	112	108	107	108	108	111	110	109	108	108	108	110
S5	0.166	173	169	169	172	169	169	171	168	168	168	168	172
S6	0.155	113	105	106	107	109	109	110	108	106	108	107	111

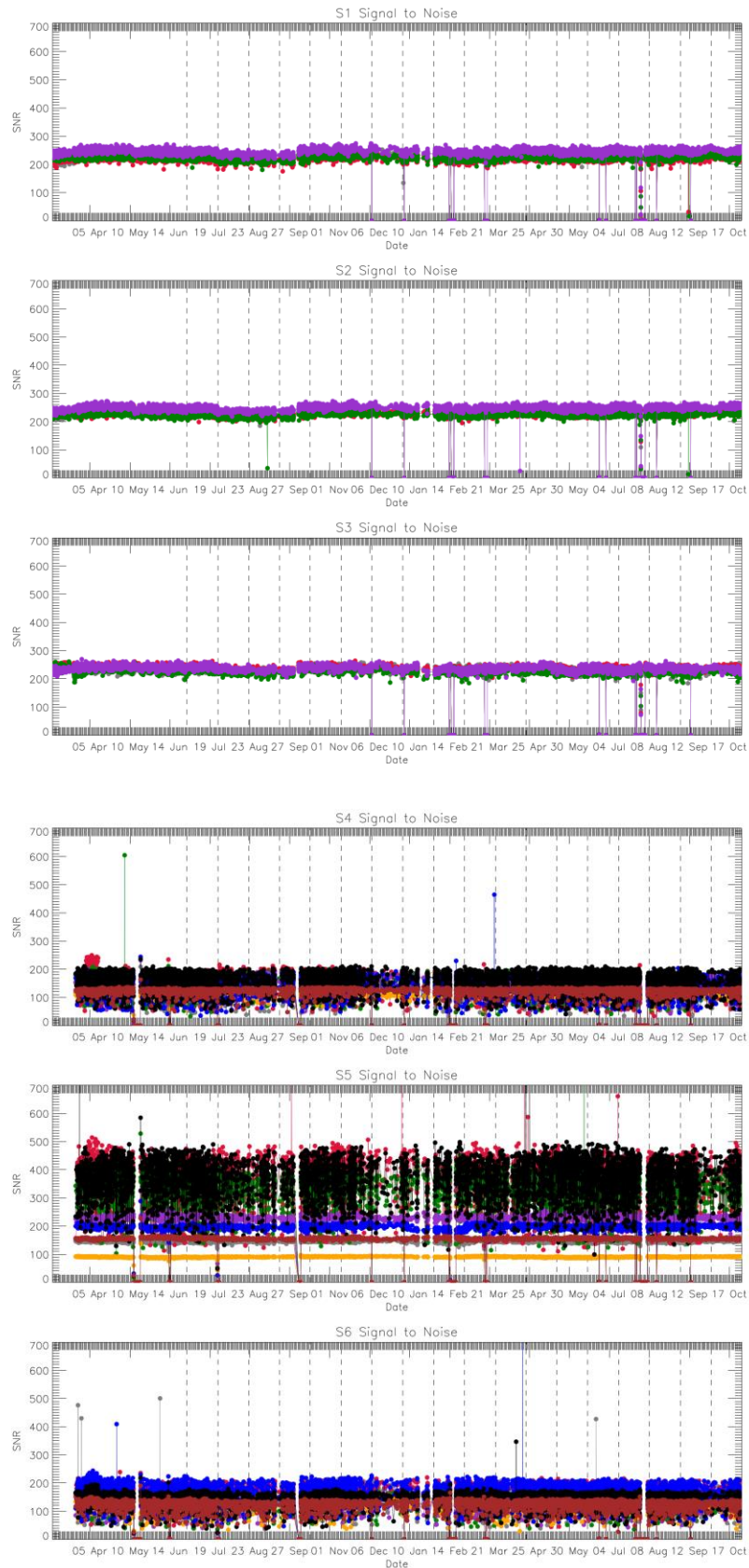


Figure 7: VIS and SWIR channel signal-to-noise of the measured VISCAL signal in each orbit. Different colours indicate different detectors.



Sentinel-3 MPC  
S3-A SLSTR Cyclic Performance Report  
Cycle No. 023

Ref.: S3MPC.RAL.PR.02-023  
Issue: 1.0  
Date: 06/11/2017  
Page: 9

### 1.3.2 TIR channel NEDT

The thermal channel NEDT values are consistent with previous operations and within the requirements. NEDT values for each cycle, averaged over all detectors and both Earth views, are shown in Table 3 and Table 4.

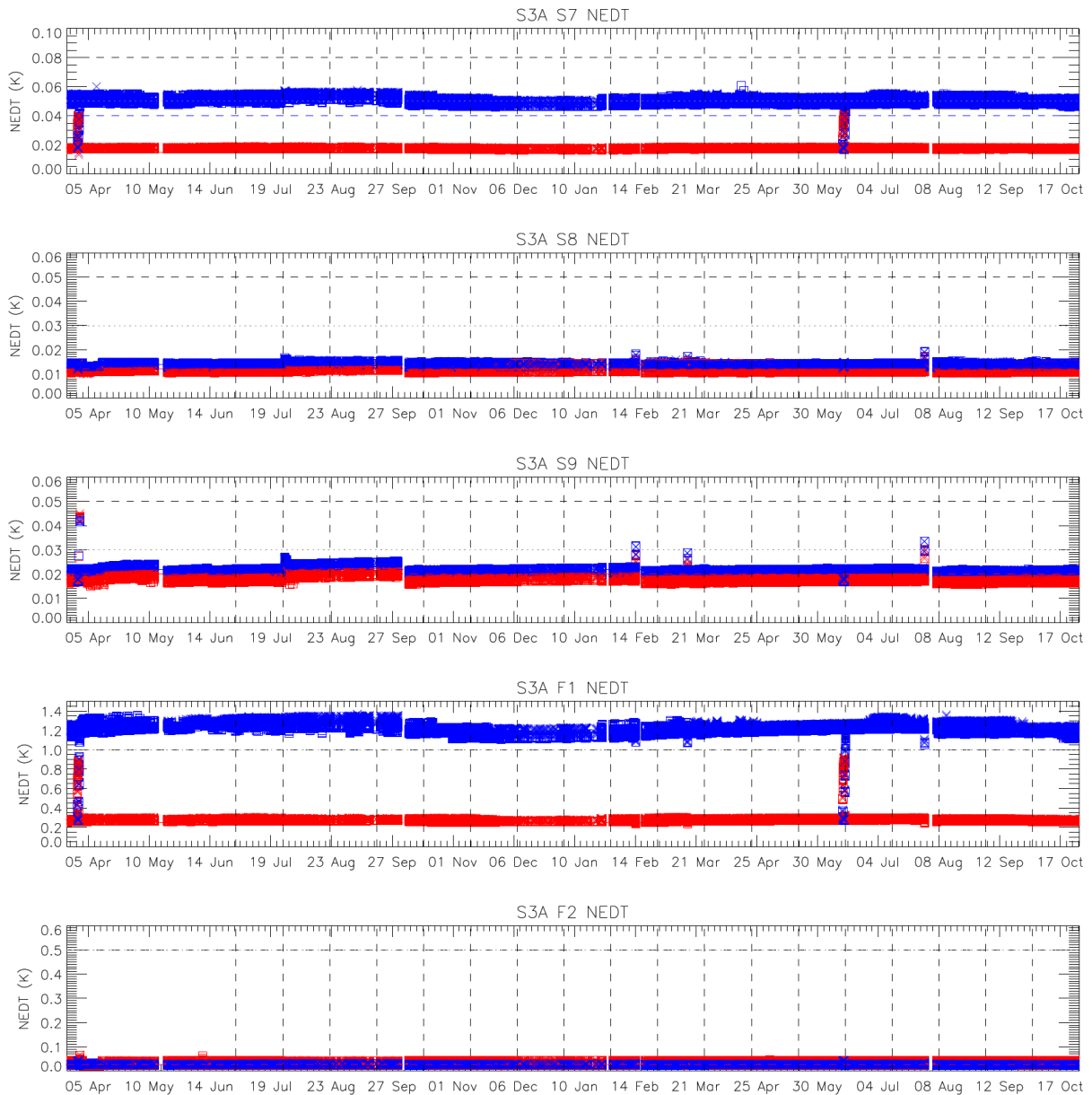


**Figure 8: NEDT trend for the thermal channels. Blue points were calculated from the cold blackbody signal and red points from the hot blackbody. Horizontal lines indicate the requirement (dashed) and goal (dotted) as well as the measured values on ground (red and blue dashed).**



**Sentinel-3 MPC**

**S3-A SLSTR Cyclic Performance Report**

**Cycle No. 023**

Ref.: S3MPC.RAL.PR.02-023

Issue: 1.0

Date: 06/11/2017

Page: 10

**Table 3: NEDT for cycles 012-023 averaged over all detectors for both Earth views towards the +YBB (hot).**

	Cycle 012	Cycle 013	Cycle 014	Cycle 015	Cycle 016	Cycle 017	Cycle 018	Cycle 019	Cycle 020	Cycle 021	Cycle 022	Cycle 023
<b>+YBB temp (K)</b>	303.680	303.621	303.206	302.674	302.544	302.541	302.593	302.386	302.348	302.307	302.479	303.116
<b>NEDT (mK)</b>												
<b>S7</b>	16.9	16.8	16.9	17.2	17.2	17.2	18.1	17.2	17.2	17.1	17.2	16.9
<b>S8</b>	11.0	11.1	11.0	10.9	10.9	11.0	11.1	11.0	11.1	10.9	10.9	10.9
<b>S9</b>	17.7	17.9	17.6	17.0	17.0	17.2	17.5	17.4	17.5	16.7	16.9	17.0
<b>F1</b>	260	260	260	268	268	271	297	276	276	269	270	265
<b>F2</b>	28.0	28.0	27.9	27.6	27.6	27.8	27.8	27.8	27.8	27.3	27.6	27.7

**Table 4: NEDT for cycles 012-023 averaged over all detectors for both Earth views towards the -YBB (cold).**

	Cycle 012	Cycle 013	Cycle 014	Cycle 015	Cycle 016	Cycle 017	Cycle 018	Cycle 019	Cycle 020	Cycle 021	Cycle 022	Cycle 023
<b>-YBB temp (K)</b>	266.512	266.353	265.807	265.183	265.136	265.260	265.412	265.125	265.000	264.902	265.032	265.779
<b>NEDT (mK)</b>												
<b>S7</b>	46.6	46.8	47.9	48.7	49.0	48.8	46.9	49.1	49.5	49.5	49.0	47.6
<b>S8</b>	14.5	14.4	14.4	14.2	14.2	14.3	14.2	14.3	14.4	14.2	14.1	14.2
<b>S9</b>	22.2	22.4	22.1	21.3	21.4	21.6	21.6	21.9	22.0	21.1	21.3	21.4
<b>F1</b>	1123	1130	1178	1222	1191	1199	1163	1229	1235	1212	1201	1162
<b>F2</b>	29.6	29.6	29.6	29.2	29.3	29.3	29.4	29.6	29.7	29.2	29.2	29.3





## 1.4 Calibration factors

### 1.4.1 VIS and SWIR VISCAL signal response

Signals from the VISCAL source for the VIS channels show oscillations due to the build up of ice on the optical path within the FPA. Decontamination must be carried out periodically in order to warm up the FPA and remove the ice. The latest decontamination cycle was successfully performed at the end of Cycle 20. The VISCAL signal has behaved as expected following the decontamination.

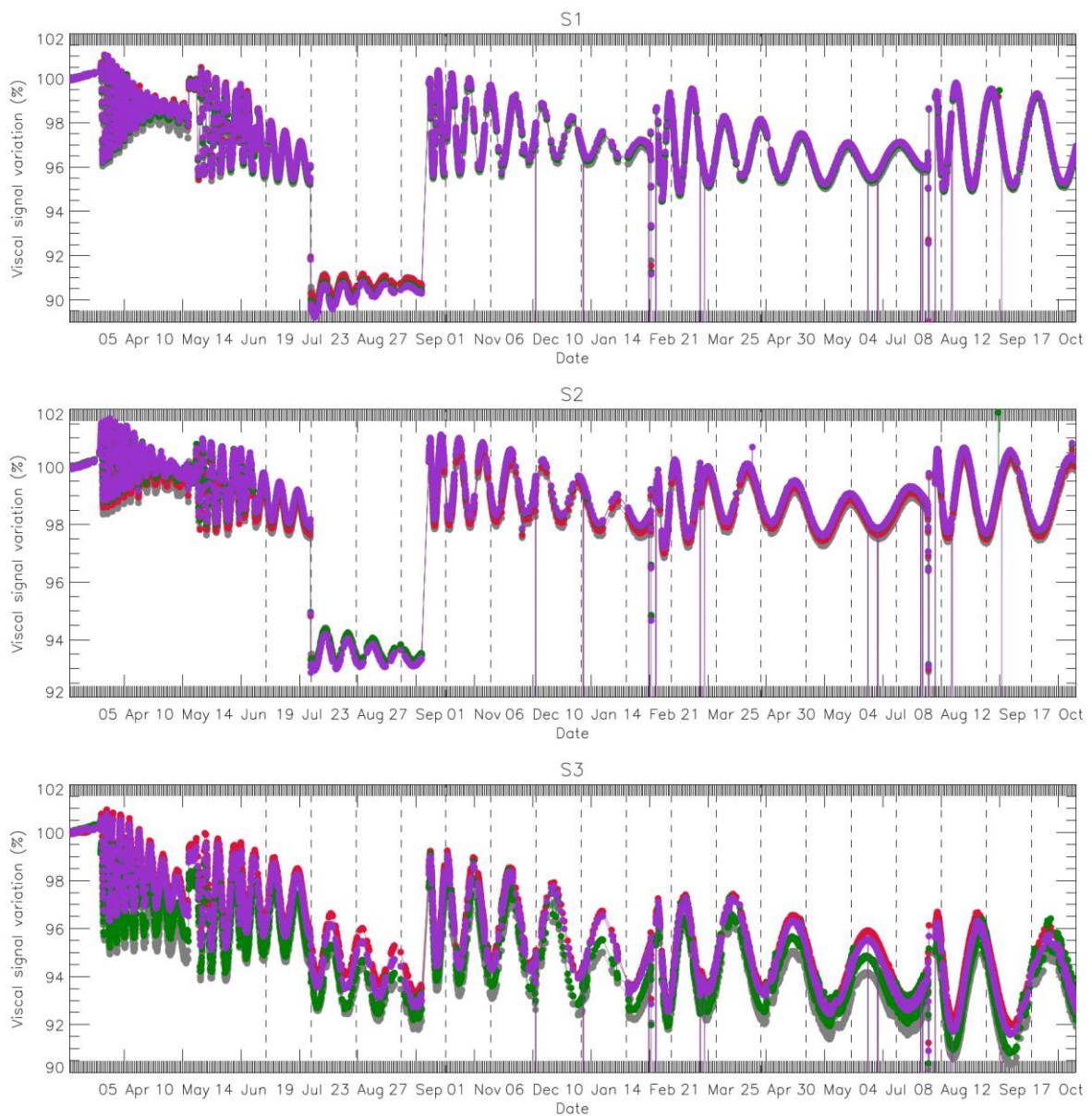


Figure 9: VISCAL signal trend for VIS channels (nadir view).

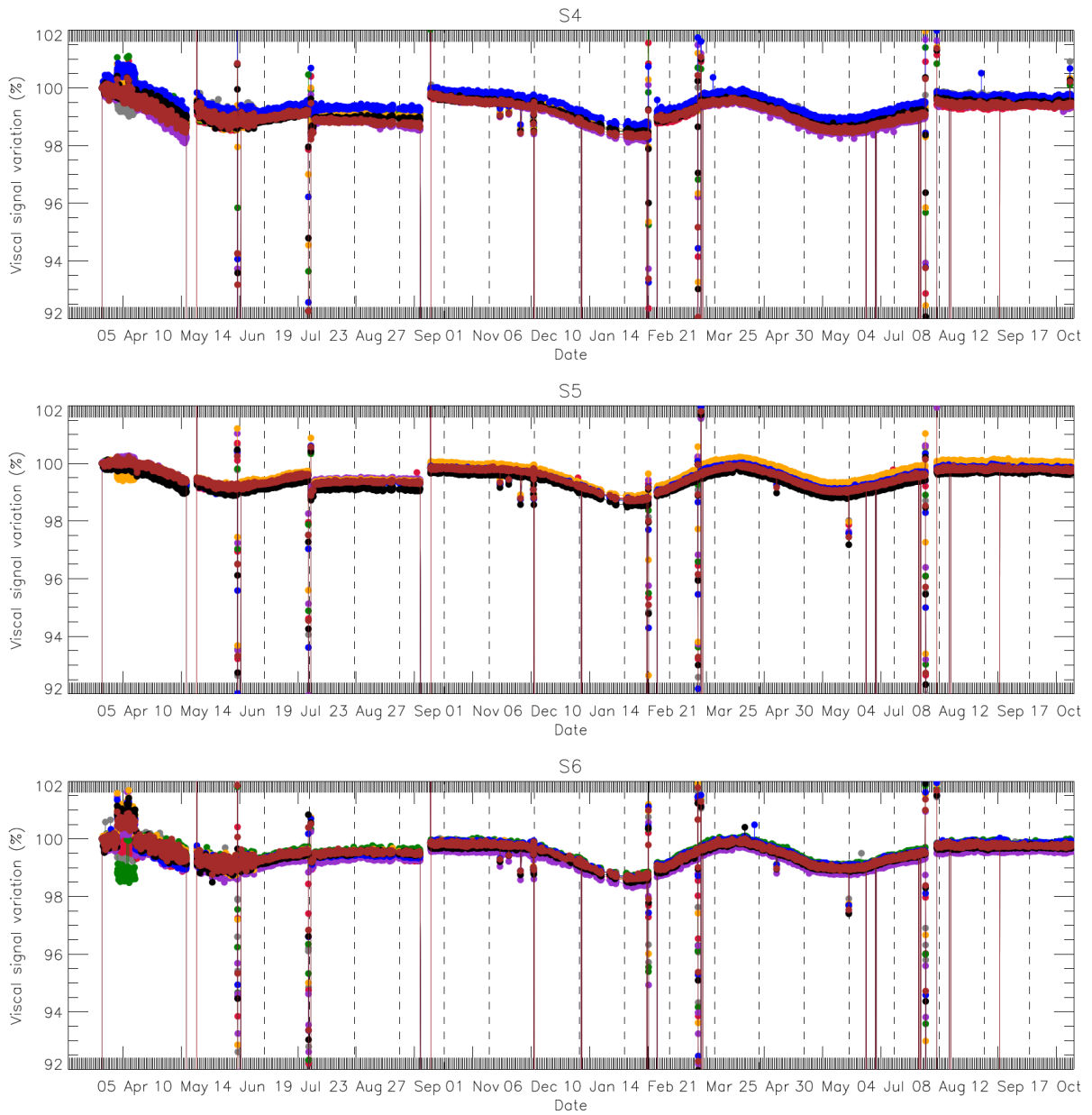


Figure 10: VISCAL signal trend for SWIR channels (nadir view).



## 2 Level 2 SST validation

Level 2 WCT SSTs have been validated using CMEMS *in situ* data for Cycle 23. Match-ups between SLSTR and *in situ* data are provided by the EUMESAT OSI-SAF.

### 2.1 Dependence on latitude, TCWV, Satellite ZA and date

- ❖ The dependence of the difference between SLSTR  $SST_{skin}$  and drifting buoy  $SST_{depth}$  for Cycle 23 is shown in Figure 11. No adjustments have been made for difference in depth or time between the satellite and *in situ* measurements. SLSTR SSTs are extracted from the SL\_2\_WCT files. Daytime 2-channel (S8 and S9) results are shown in red, night time 2-channel results are shown in blue and night time 3-channel results are shown in green. Solid lines indicate dual-view retrievals, dashed lines indicate nadir-only retrievals. Bold lines indicate statistically significant (95% confidence) results.

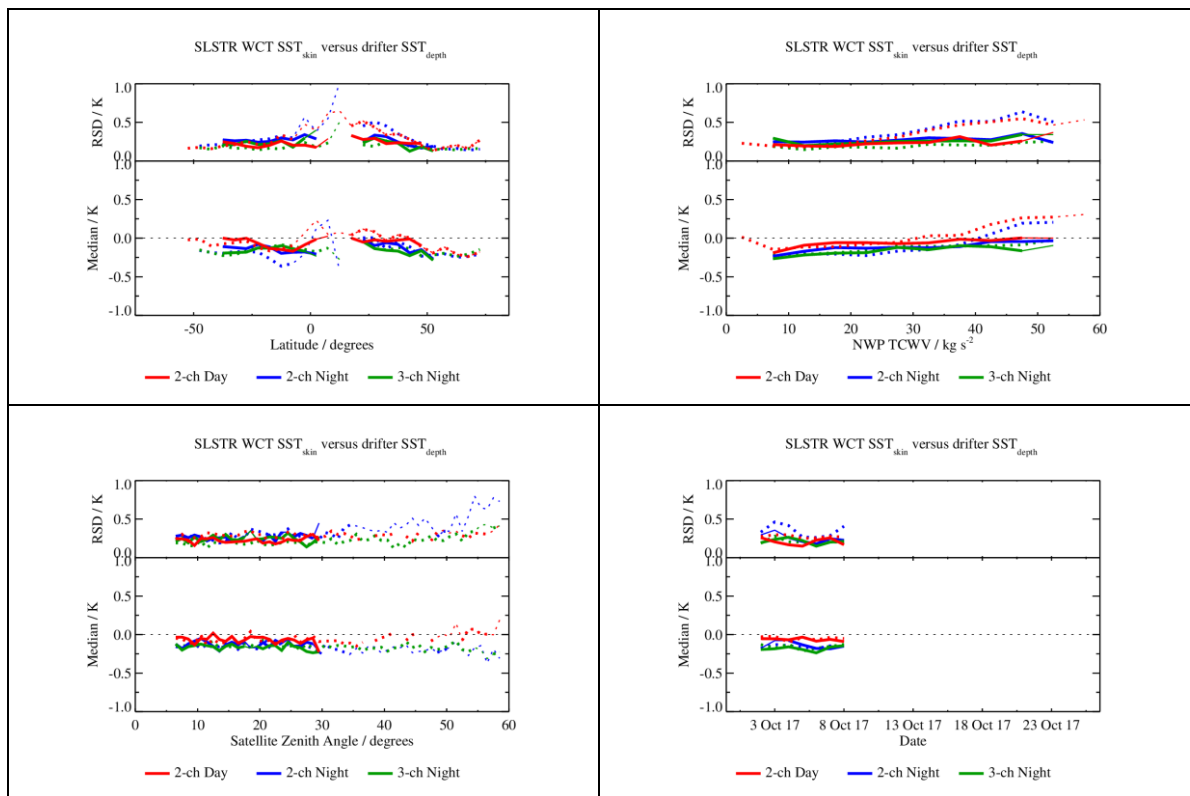


**Figure 11: Dependence of median and robust standard deviation of match-ups between SLSTR  $SST_{skin}$  and drifting buoy  $SST_{depth}$  for Cycle 23 as a function of latitude, total column water vapour (TCWV), satellite zenith angle and date. The data gap towards the end of the cycle is due to a delay in match-up production.**



## 2.2 Spatial distribution of match-ups

- ❖ The spatial distribution of SLSTR/drifter match-ups for Cycle 23 is shown in Figure 12. No adjustments have been made for difference in depth or time between the satellite and *in situ* measurements.

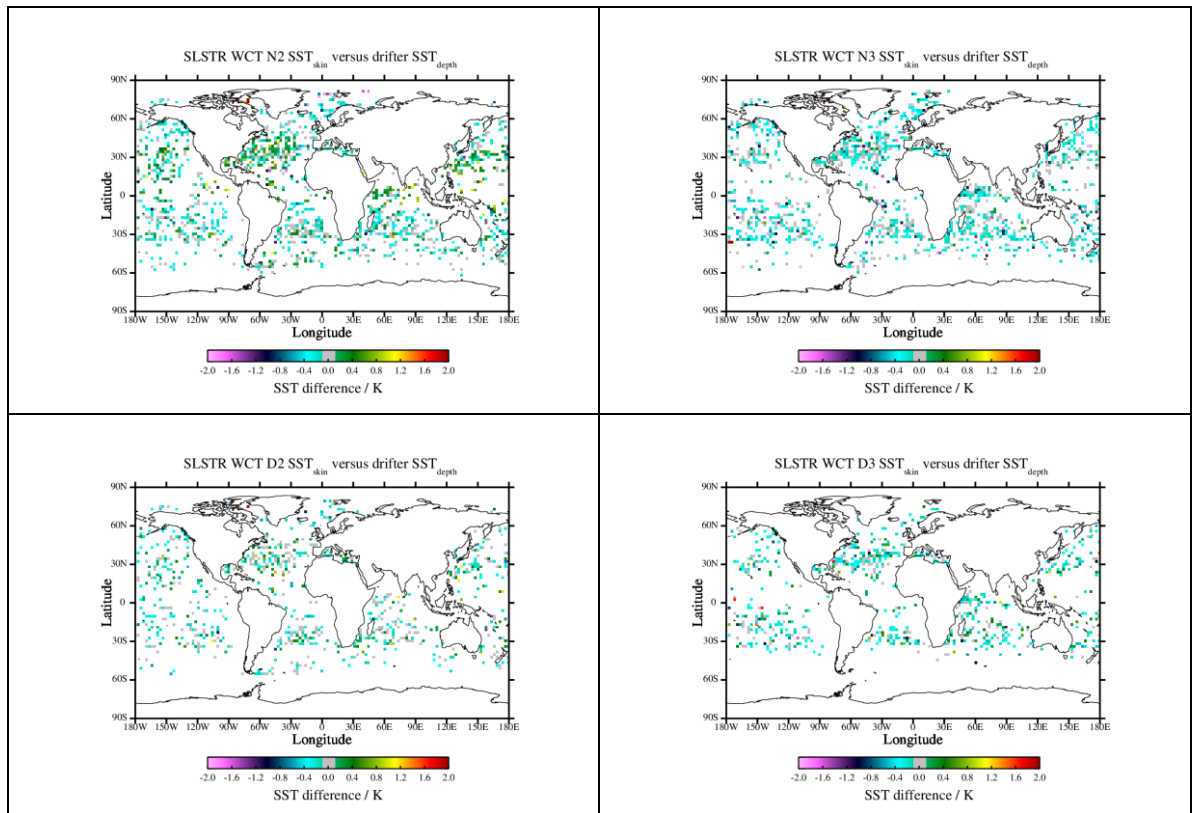


Figure 12: Spatial distribution of match-ups between SLSTR  $SST_{skin}$  and drifting buoy  $SST_{depth}$  for Cycle 23.



## 2.3 Match-ups statistics

- ❖ Match-ups statistics (median and robust standard deviation, RSD) of SLSTR/drifter match-ups for Cycle 23 is shown in Table 5. No adjustments have been made for difference in depth or time between the satellite and *in situ* measurements and so at night time (in the absence of diurnal warming) an offset of around -0.17 K is expected. The RSD values indicate SLSTR is providing SSTs mostly within its target accuracy (0.3 K).

**Table 5: SLSTR drifter match-up statistics for Cycle 23.**

Retrieval	Number	Median (K)	RSD (K)
N2 day	3338	-0.06	0.29
D2 day	1475	-0.06	0.23
N2 night	3457	-0.17	0.33
N3 night	3457	-0.15	0.21
D2 night	1383	-0.12	0.28
D3 night	1383	-0.16	0.24



### 3 Level 2 LST validation

Level 2 Land Surface Temperature products have been validated against *in situ* observations (Category-A validation), and intercompared (Category-C validation) with respect to three independent reference products from the ESA DUE GlobTemperature Project (MODIS, GOES, and SEVIRI).

#### 3.1 Category-A validation

Category-A validation uses a comparison of satellite-retrieved LST with *in situ* measurements collected from radiometers sited at a number of stations spread across the Earth, for which the highest-quality validation can be achieved. The results can be summarised as follows (see Figure 13 and Figure 14):

- ❖ Average absolute accuracy (vs. Gold Standard):
  - Daytime: 0.81K
  - Night-time: 1.07K

This daytime accuracy meets the mission requirement of < 1K. The night-time accuracy is very close to this mission requirement. This also is in line with the GCOS climate requirements of 1 K accuracy.

- ❖ Average precision (vs. Gold Standard):
  - Daytime: 0.72K
  - Night-time: 1.21K

While there is no Sentinel-3 mission requirement for precision, the daytime precision meets the GCOS climate requirement of 1K. The night-time accuracy is also very close to this climate requirement.

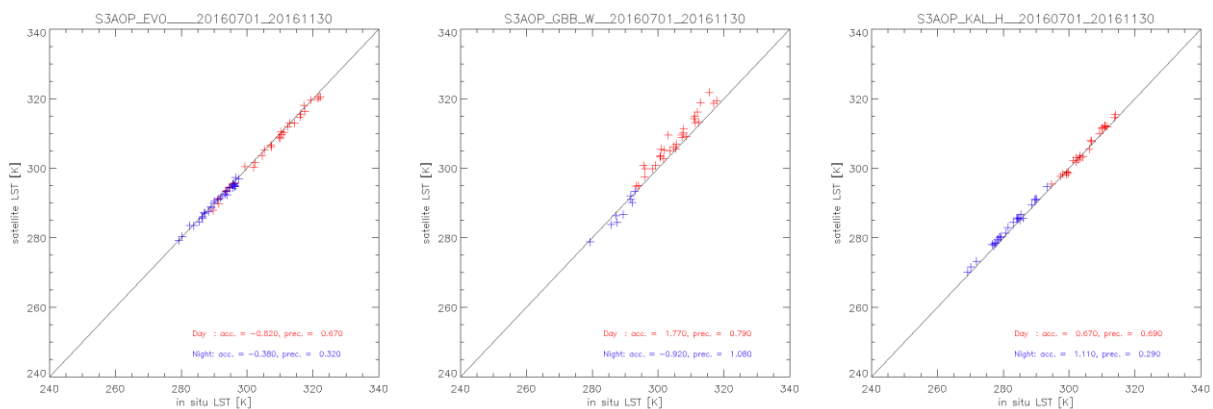
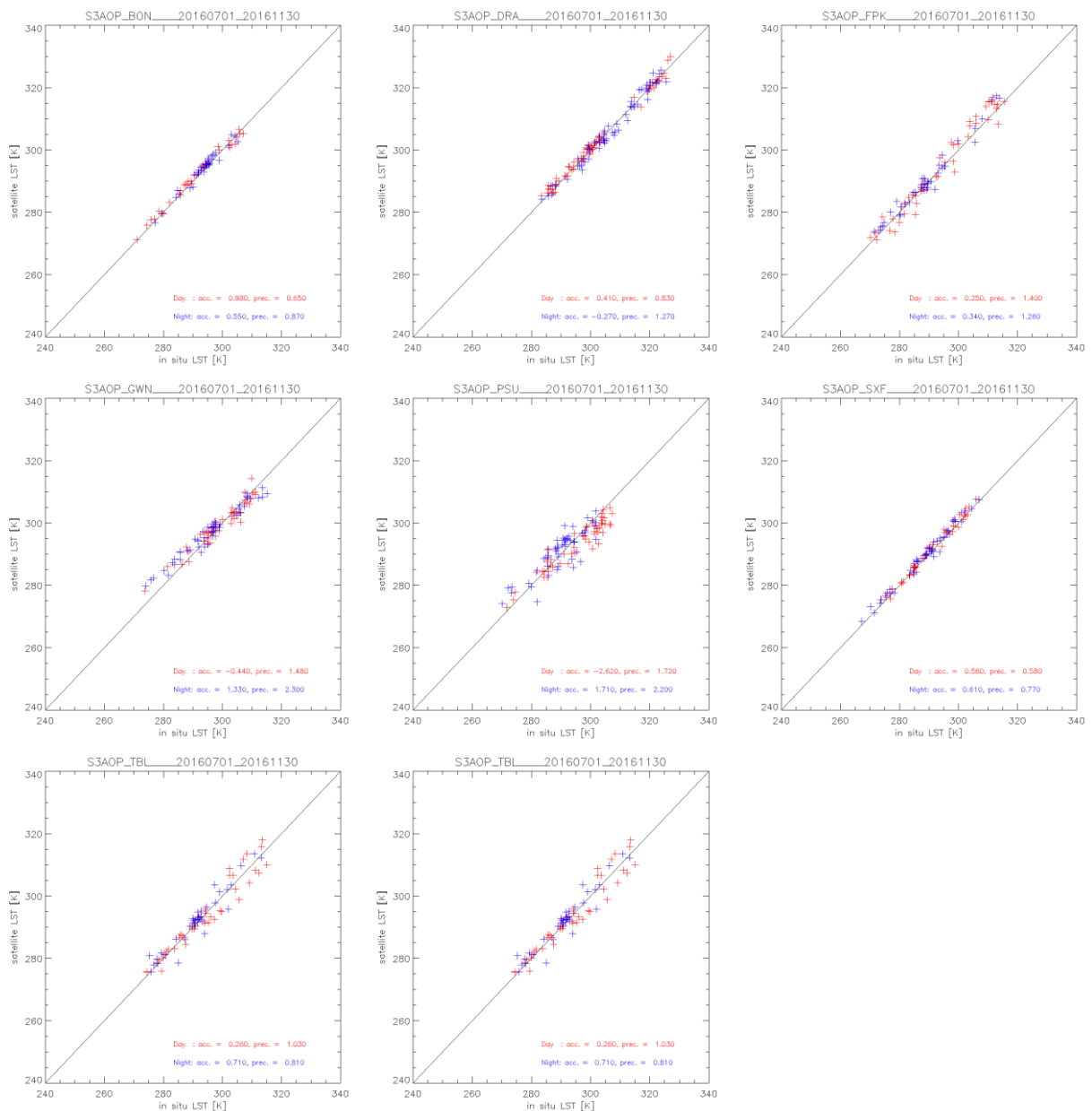



Figure 13: Validation of the SL\_2\_LST product over the mid-July to mid-November reprocessed period at three Gold Standard *in situ* stations managed by the Karlsruhe Institute of Technology: Evora, Portugal (left); Gobabeb, Namibia (centre); Kalahari-Heimat, Namibia (right). [Results courtesy of Maria Martin through the GlobTemperature Project]



**Figure 14: Validation of the SL<sub>2</sub>LST product over the mid-July to mid-November reprocessed period at the seven Gold Standard in situ stations of the SURFRAD network plus a Gold Standard station from the ARM network: Bondville, Illinois top-(left); Desert Rock, Nevada (top-centre); Fort Peck, Montana (top-right); Goodwin Creek, Mississippi (middle-left); Penn State University, Pennsylvania (middle-centre); Sioux Fall, South Dakota (middle-right); Table Mountain, Colorado (bottom-left); and Southern Great Plains, Oklahoma (bottom-centre).**

	<p><b>Sentinel-3 MPC</b></p> <p><b>S3-A SLSTR Cyclic Performance Report</b></p> <p><b>Cycle No. 023</b></p>	<p>Ref.: S3MPC.RAL.PR.02-023</p> <p>Issue: 1.0</p> <p>Date: 06/11/2017</p> <p>Page: 18</p>
--	---	--

## 3.2 Category-C validation

---

Category-C validation uses inter-comparisons with similar LST products from other sources such as AATSR, AVHRR, MODIS, SEVIRI, and VIIRS, which give important quality information with respect to spatial patterns in LST deviations. The results can be summarised as follows:

- ❖ Daytime intercomparison differences are: ~1K vs. GOES\_\_LST\_2 over North America; ~1K vs. SEVIR\_LST\_2 over Europe; and < 1K vs. MOGSV\_LST\_2 on a Global basis.
- ❖ Night-time intercomparison differences are: <1K vs. GOES\_\_LST\_2 over North America; <1K vs. SEVIR\_LST\_2 over Europe; and < 1K vs. MOGSV\_LST\_2 on a Global basis.
- ❖ Differences with respect to biomes tend to be larger during the day for surfaces with more heterogeneity and/or higher solar insolation. With respect to SLSTR zenith viewing angle differences are larger in the day on the left side of the SLSTR swath in the along-track direction.






## 4 Events

SLSTR was switched on and operating nominally during the cycle, with SUE scanning and autonomous switching between day and night modes. However, a short loss of data occurred during downlink to the ground station on the 25<sup>th</sup> October 2017 due to radio frequency interference with another satellite. This resulted in a period of compromised data for up to 5 minutes in the Level-1 and Level-2 images, affecting the visible channels from approximately 10:31:40 and the infrared channels from 10:33:20. All channels returned to normal by 10:36. An example Level-1 image showing the start of the affected region for visible and infrared channels is given in Figure 15.

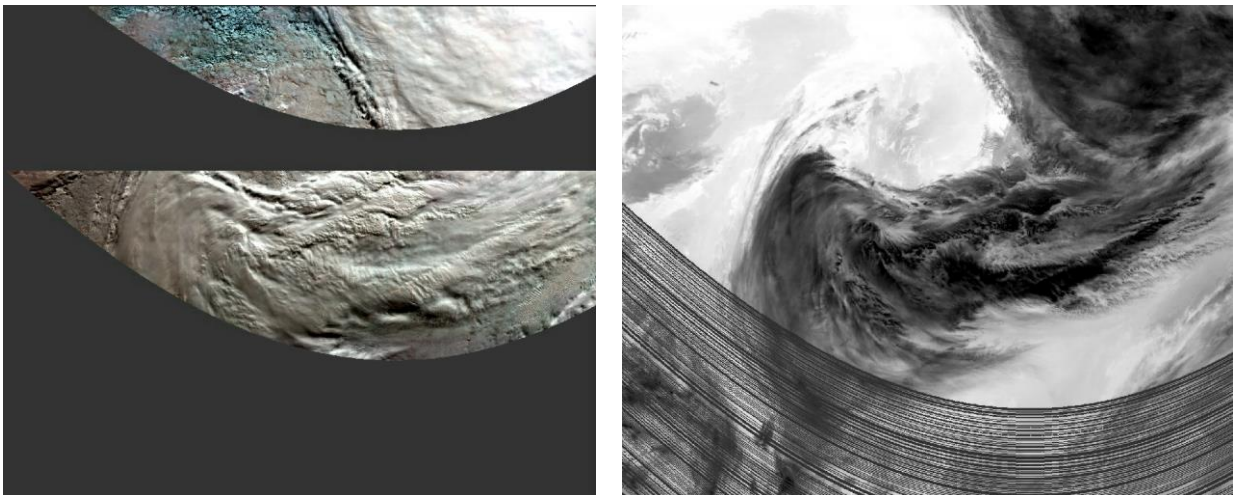


**Figure 15: Level-1 image for visible channels (left) with S1 blue, S2 green and S3 red, and for S8 (right) on 25<sup>th</sup> October 2017 for the granule starting at 10:30. The affected area starts at 10:31 in the visible channels and at 10:33 in the infrared channels.**

 The logo for the Sentinel-3 Mission Performance Centre. It features a blue satellite icon at the top, the text 'SENTINEL 3' in blue, and 'Mission Performance Centre' in blue. Below the text are four small square images: a sunset, a satellite, a landscape, and a person. A green checkmark is at the bottom right.	<b>Sentinel-3 MPC</b> <b>S3-A SLSTR Cyclic Performance Report</b> <b>Cycle No. 023</b>	Ref.: S3MPC.RAL.PR.02-023 Issue: 1.0 Date: 06/11/2017 Page: 20
--	--	---

## 5 Appendix A

Other reports related to the Optical mission are:

- ❖ S3-A OLCI Cyclic Performance Report, Cycle No. 023 (ref. S3MPC.ACR.PR.01-023)

All Cyclic Performance Reports are available on MPC pages in Sentinel Online website, at:  
<https://sentinel.esa.int>

*End of document*